Modeling and Optimization of Displacement Windings for Transformers in Dual Active Bridge Converters

Shen, Zhan; Shen, Yanfeng; Qin, Zian; Wang, Huai

Important note
To cite this publication, please use the final published version (if applicable).
Please check the document version above.

Modeling and Optimization of Displacement Windings for Transformers in Dual Active Bridge Converters

Zhan Shen[*], Yanfeng Shen[*], Zian Qin[†], and Huai Wang[*]

zhs@et.aau.dk, yaf@et.aau.dk, Z.Qin-2@tudelft.nl, hwa@et.aau.dk

[*]Department of Energy Technology, Aalborg University, Aalborg, Denmark

[†]Department of Electrical Sustainable Energy, Delft University of Technology, Delft, Netherlands

Abstract— **The transformer in the dual active bridge converter (DAB) is the key element which provides galvanic insulation and voltage conversion. The parasitic parameters, including winding capacitance, ac resistance, and leakage inductance, are the primary considerations in its winding design. Without proper consideration of those parameters could result in issues on current ringing, high power loss, and overheating. In this paper, a comprehensive study is devoted to those parameters. A winding design method is presented by taking all those parameters into consideration. Special attention is paid to the impact of displacement winding, which is quite often in the manufacture and especially in prototype design phase. Both the normal and displacement winding will be studied and compared, with analytical, simulation, and experimental methods. Through comparison, additional coefficients are introduced to the simple analytical equations so that they could also be applied for displacement windings. Several considerations are given to control those parameters within a reasonable range in the design and manufacture phase. Finally, the analysis and design method are verified by finite element method and the experimental results on a 120 kHz prototype, and can be extended to other high-frequency magnetic designs.**

Fig. 1. A dual active bridge converter (DAB).

Fig. 2. Transformer cross-section and parameter definitions.

I. INTRODUCTION

The parasitic parameters of the transformer winding, e.g. capacitances, ac resistance, and leakage inductance, have significant impact on the performance of the dual active bridge converter (DAB) [1–3]. A high winding capacitance could cause severe current ringing and capacitive switching losses [4–6]. The efficiency of the transformer mainly depends on the core and resistive losses, the latter is directly related the efforts to minimizing the ac resistance [7, 8]. A certain leakage inductance is essential to the required power transfer and current shaping [1, 9]. Thus, a well predicted and optimized winding structure is important for the transformer design.

In this paper, a winding design method for the transformer is proposed considering capacitances, ac resistance and leakage inductance. The impact of the difference between the nor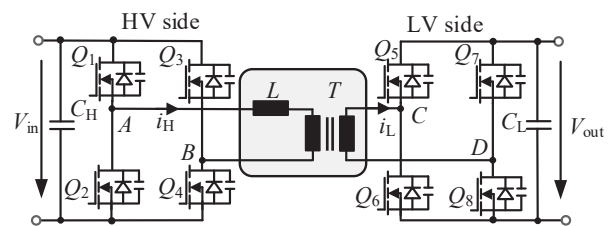mal and displacement winding is investigated through the comparison of analytical, finite element method and experimental results. The comparison results can help engineers to use simple analytical model for displacement winding with modification coefficients, and to choose winding configurations from perspective of parasitic parameters control. Then followed by a pre-design of leakage inductance, the winding capacitance and ac resistance are optimized in a two-dimensional plane through Pareto optimization. Finally, the transformer for a 120 kHz DAB converter is designed to verify the proposed method.

II. IMPACT OF DISPLACE ORDER WINDING

The position of the winding in magnetics is difficult to fix in manufacture. Initially, the winding is designed as Fig 3. (a, b). With the tolerance errors, the winding is less likely to keep organized, and turns to the structure in Fig 3. (c, d). The displacement becomes serious with the increase of the
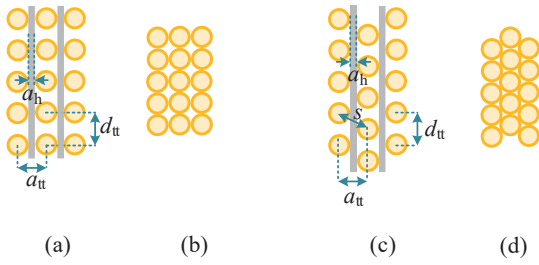
Fig. 3. Different winding placement positions (a) orthogonal winding, (b) compact orthogonal winding, (c) orthocyclic winding, (d) compact orthocyclic winding. The former two are defined as normal windings, and the latter two are defined as displacement windings.

Fig. 4. The relation between radius ratio, permittivity, and displacement capacitance ratio

number of turns and layers, especially in high voltage ratio transformer. Moreover, sometimes in the compact winding design, the compact orthogonal (b) and compact orthocyclic windings (d), are applied on purpose to reduce the cost of layer insulation to achieve high window utilization factor and high power density. In the aspect of winding width (in a_{tt} direction), the width increment of the normal winding is d_e, while the orghocyclic winding is $\frac{\sqrt{3}}{2}d_e$, which is 13.4% less and thereby leads to a smaller volume of the winding. Besides, the impact of the displacement to various parameters is detailed discussed below.

A. Impact on winding capacitance

The cylindrical and parallel plate capacitance models $C_{l,p}$ are two most basic models for analytical calculation, the former is given as:

$$C_{l,c} = \varepsilon_0 \varepsilon_i \frac{2\pi h}{\ln(1 + d/r)}, \tag{1}$$

and the later is given as:

$$C_{l,p} = \varepsilon_0 \varepsilon_i \frac{2\pi h(r + d/2)}{d}, \tag{2}$$

where ε_0 and ε_i are vacuum permittivity and relative permittivity of insulation material, separately. They could also be used to model the capacitance between the winding layers by applying $d = d_{eff}$ as the effective insulation distance for orthogonal winding [10] (c.f. Fig 3 (a)):

$$d_{eff} = d_e + h - 2.3 \cdot r_i + 0.26 \cdot d_{tt}. \tag{3}$$

The displacement could introduce a large distribution of capacitance values [11]. The electric field of orthocyclic windings is different from the orthogonal winding, and the layer capacitance for those is given in [12]:

$$C_{l,m} = t\varepsilon_0 \frac{4\varepsilon_r \arctan\left[\frac{(\sqrt{3}-1)(2\varepsilon_r + k_{ln})}{(\sqrt{3}+1)\sqrt{k_{ln}(2\varepsilon_r + k_{ln})}}\right]}{\sqrt{2\varepsilon_r k_{ln} + k_{ln}^2}} \tag{4}$$

where $k_{ln} = \ln k_{rad}$, $k_{rad} = d_e/d_i$ is the radius ratio, t is the number of turns per layer.

The displacement capacitance ratio is defined for the comparison of the orthogonal and orthocyclic winding:
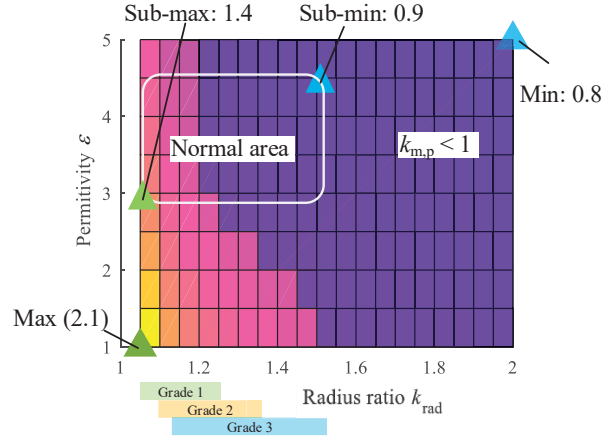
$$k_{m,p} = \frac{C_{l,m}}{C_{l,p}} \tag{5}$$

TABLE I
RADIUS AND DISPLACEMENT CAPACITANCE RATIO OF DIFFERENT WIRE GRADES

Grade	Radius ratio k_{rad}	Displacement capacitance ratio $k_{m,p}$
1	$1.05 \sim 1.24$	$1.48 \sim 0.99$
2	$1.09 \sim 1.37$	$1.28 \sim 0.94$
3	$1.13 \sim 1.54$	$1.19 \sim 0.89$

The relationship between $k_{m,p}$ and k_{rad} is illustrated in Fig. 4. The maximum value occurs at the low permittivity and radius ratio, while the minimum value vise verse. The upper right corner covered by purple color is those situations with $k_{m,p}$ smaller than 1. To have a further impression of the comparison, the enameled copper wire from Elektrisola is chosen to calculate the radius ratio range [13]. The diameter is from 0.01 mm to 0.5 mm according to IEC 60317. Normally, ε of insulation material is between 3 and 4.5. Combing those two boundaries, we could obtain a normal area in Fig. 4. The color bar under the axis illustrates the detailed radius ratio distribution of different grades. The detailed result of different displacement capacitance ratio $k_{m,p}$ is given in Table I. For large grade and thicker insulation, the displacement helps decrease the parasitic capacitance. For lower grade and thin insulation which is more common, the increase of capacitance due to displacement is very serious. Thus, an empirical coefficient could be introduced according to Table I when using simple parallel plate capacitance to predict the displacement orthocyclic winding. In order to reduce the capacitance due to the displacement, one solution is to add insulation layer between layers (Fig. 3 (a, c)), another is to use high-grade wires with thicker insulation. Although all of the three grades of wires have the similar lowest displacement capacitance ratio $k_{m,p}$ close to 0.9, using the high-grade insulation wire could ensure that the capacitance increase ratio due to the displacement could only reach 1.19, which is far below the Grade 1 wire. The above two solutions all focus on increasing

1926

TABLE II
PARAMETERS OF INDUCTORS BUILT FOR COMPARISON

Parameters	Value	Units
Core type	ETD 59/31/22	
Core material	N97	
Bobbin type	B66398	
Pri. Number of layers p	3	
Sec. Number of layers p	3	
Turns per layer t	34	
Conductor diameter d	1	mm
Insulation coating r_{iso}	0.05	mm
Insulation distance a_{iso}	1.2	mm

Fig. 6. Comparison of ac resistance R_{ac} in normal and displacement winding.

Fig. 5. The Prototype Td with displacement winding as Fig. 3 (d).

the thickness of the insulation system, and will have additional cost in large amount production.

B. Impact on ac resistance

The classic ac resistance model is derived with the assumption of ordered conductor placement and one-dimensional field distribution[16, 17], Dowell's equation for the winding ac resistance R_{ac} is:

$$R_{\text{ac}} = R_{\text{dc}}F_{\text{r}}, \qquad (6)$$

with

$$F_{\text{r}} = \triangle[\nu_3 + \frac{2}{3}(m^2 - 1)\nu_2] \qquad (7)$$

and

$$\nu_2 = \frac{\sinh\triangle - \sin\triangle}{\cosh\triangle + \cos\triangle}, \quad \nu_3 = \frac{\sinh(2\triangle) + \sin(2\triangle)}{\cosh(2\triangle) - \cos(2\triangle)}, \quad (8)$$

where R_{dc} and R_{dc} are the winding ac and dc resistance, F_{r} is the winding resistance factor, v_3, v_2 are high-frequency coefficients related to skin and proximity effect, and m is the number of layers, the penetration ratio $\triangle$ is calculated by:

$$\triangle = \frac{d_{\text{i}}}{\delta}, \qquad (9)$$

where d_{i} is the conductor diameter and δ is skin depth. With the equation above, there is no typical information of winding position included to predict the ac resistance. The difference
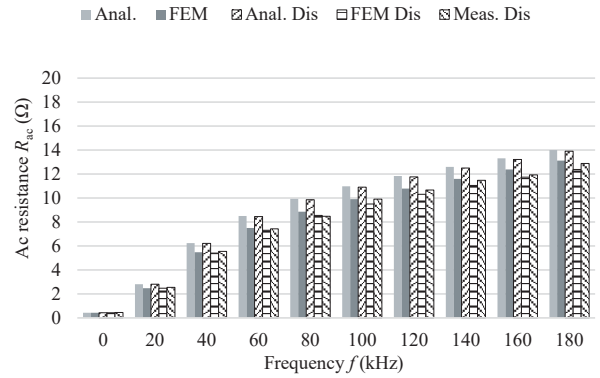
of mean length per turn (MLT) of normal and displacement winding can cause a small difference in their ac resistance. Normally, it takes more wire in the process of wiring for normal winding, so its MLT and ac resistance is slightly larger.

In order to illustrate the impact of displacement winding on the ac resistance and leakage inductance, two transformers Prototypes named Td and Tn are designed, analytically calculated and simulated. The former is with the displacement winding and the later is with the normal winding. They have three layers for primary and secondary, separately. Only Prototype Td is built due to that wiring the normal compact orthogonal winding by hand is very difficult. The specification of the core and bobbin are listed in Table II. The number of turns per layer t is 34 to reduce the impact of fringe effect [15]. Their comparison of ac resistance R_{ac} is given in Fig. 6. The results of the normal winding are given named Anal., FEM, and displacement winding are given named Anal. Dis., FEM Dis. and Meas. Dis.. All of the analytical, finite elemental model and experimental results shows that the displacement has no too much impact on the ac resistance in each frequency. The magnetic field keep straight in most places in both two cases due to their compact structure, thus no too much difference is introduced. The small difference in two cases is due to their small difference in MLT and hand-wiring process.

C. Impact on ac leakage inductance

The ac leakage inductance is to illustrate the energy storage ability of the winding structure [9, 16, 18, 19]:

$$L_\sigma = \mu_0 m_1^2 \frac{l_{\text{w}}}{h_c}(\underbrace{d_{w1}\frac{m_1}{3}F_{L1} + d_{w2}\frac{m_2}{3}F_{L2}}_{\text{frequency dependent}}$$
$$\underbrace{+ d_g + d_{i1}\frac{m_1 - 1}{2m_1} + d_{i2}\frac{m_2 - 1}{2m_2}}_{\text{frequency independent}}). \qquad (10)$$

where m_1, m_2 is the layer number of primary and secondary winding; d_{w1}, d_{w2} is the thickness of two winding; d_g is the interwinding gap thickness; d_{i1}, d_{i2} is the inter-layer gap
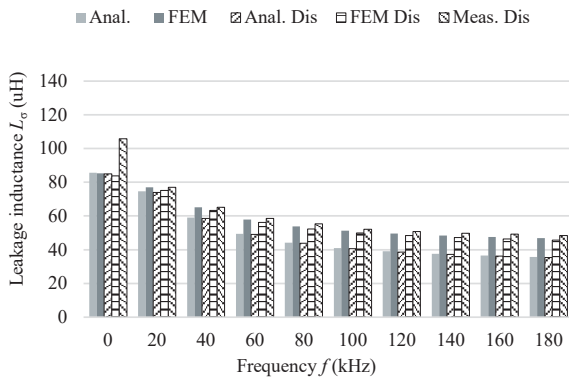
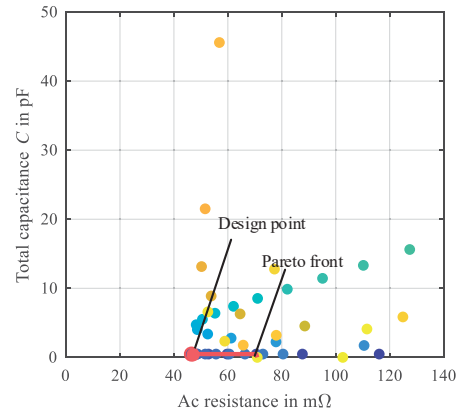Fig. 7. Comparison of ac leakage inductance L_σ in normal and displacement winding.

Fig. 8. High voltage winding design Pareto front and design point

Fig. 9. Inductor and transformer in a dual active bridge prototype.

thickness, F_L can be solved by:

$$F_{L1} = \frac{1}{2m_1^2 \triangle}[(4m_1^2 - 1)\varphi_1 - 2(m_1^2 - 1)\varphi_2]. \quad (11)$$

with

$$\varphi_1 = \frac{\sinh(2\triangle) - \sin(2\triangle)}{\cosh(2\triangle) - \cos(2\triangle)} \quad \varphi_2 = \frac{\sinh\triangle - \sin\triangle}{\cosh\triangle - \cos\triangle} \quad (12)$$

Unlike the ac resistance value which is only dependent on the magnetic field inside the conductor, the inductance value is also dependent on the air or insulation between winding layers (frequency independent part).

With the two prototypes in the last section, a comparison of ac leakage inductance L_{ac} is given in Fig. 7. Analytically, the difference between the normal and displacement winding lies in the difference of the mean length per turn (MLT), the width of each winding, which are both very small. So the difference of the analytical results in both comparisons of the two cases is neglectable. Due to the accurate control of the leakage width between primary and secondary winding, the finite element simulation and experimental results also fit the analytical model very well.

III. PARASITIC PARAMETERS WINDING DESIGN

From the comparison of the parasitic parameters in the last section, the ac resistance and leakage inductance is position-independent in the reasonable range. The winding capacitance, on the other hand, is very sensitive to the position and the displacement. For the sake of convenience in practice, the simple analytical equations (1) and (2) are corrected with the empirical coefficients in Table I to predict the winding capacitance in displacement windings. For each wire grade, the larger displacement capacitance ratio is for very compact wiring and the small ratio is for the loose design. In this way, the use of complex equations can be omitted and the accuracy of the analytical model can be guaranteed.

In [20, 21], analytical methods are proposed to optimize the ac resistance with each number of layers p. It is later developed in [22] to optimize in the (p, Δ) domain. It is also possible to implement the capacitance in the (p, Δ) domain with some pre-optimization procedure. A series inductor will
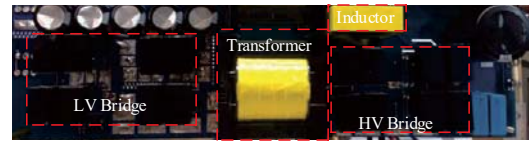
be introduced for the leakage inductance, the initial design of the transformer requires only a minimum controlled leakage inductance 300 nH. The low voltage side capacitance and core capacitance is ignored due to the transfer of turn ratio, and only the high voltage side capacitance is considered. In the preliminary design, the leakage inductance is assumed using the dc leakage inductance formula, and a minimum insulation distance a_{psiso} then can be gained, and it is set as one of the boundary conditions for the design. Further, the winding capacitance is mainly decided by the layer insulation, thus maximum layer insulation a_{iso1} and a_{iso2} are chosen for the each design. Due to the power balance, the window width for the primary and secondary side winding is set equal. The thin insulation Litz wire conductor is chosen as the conductor. Under the assumptions above, the parameters now become a two-dimensional optimization problem in (p, Δ) domain, and a global optimization could be used with the method in [22] for both ac resistance and winding capacitance.

For verification, a transformer for a 120 kHz dual active bridge prototype is designed, and the design input and output parameters are given in Table III. The relationship between C_w and R_{ac} of the high voltage winding is plotted in Fig. 8 and the Pareto front is with red line. All the points on the Pareto front is with the $p = 1$ situation, and is with no much difference in terms of capacitance. So the left side point of the Pareto front is chosen as the design point. The transformer prototype built with the optimal design is illustrated in Fig. 9. Due to the increase of chosen wire diameter, the real prototype has two layers of winding for the high voltage side. Alternatively, a comparison transformer was built with the same specification of high voltage side and the core, but with 0.2 mm foil as the
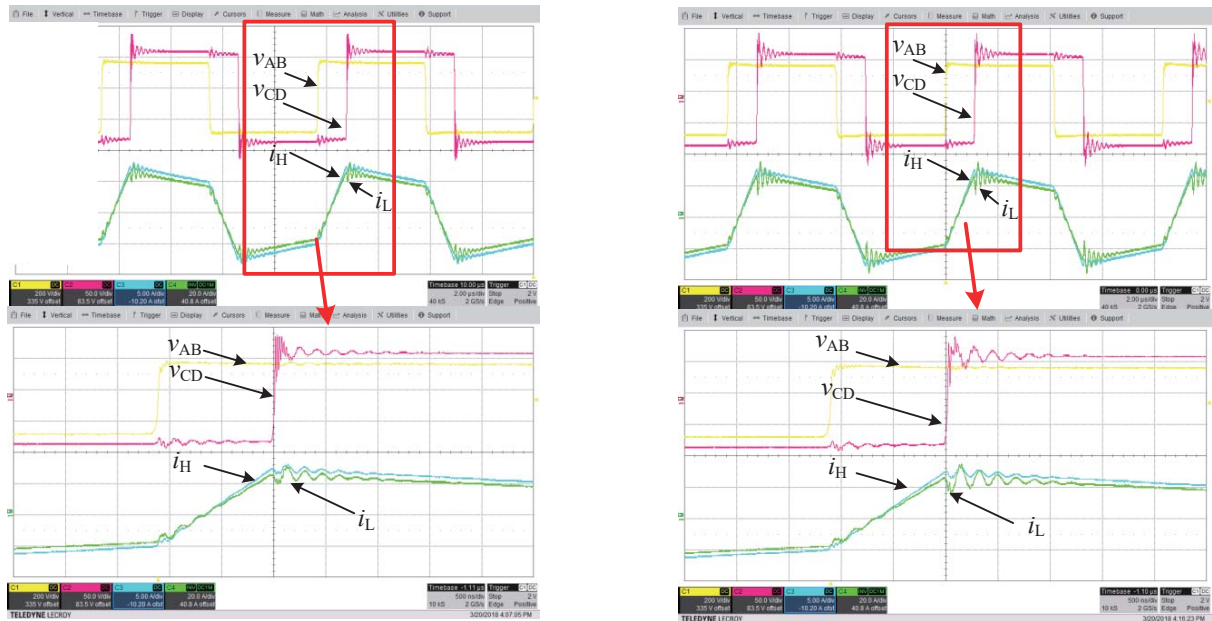
(a) Optimum designed transformer waveform.

(b) Comparison transformer waveform.

Fig. 10. Optimum design and comparison transformer operation waveform.

TABLE III
TRANSFORMER WINDING DESIGN INPUTS AND OUTPUTS

| Input Parameters | Value | | Units |
	Pri.	Sec.	
Core type	ETD 59/31/22		
Core material	N97		
Bobbin type	B66398		
Number of turns p	21	6	
Number of strands k_{str}	50		
Output Parameters			
Number of layers p	1	1	
Turns in one layer t	21	6	
d_i output	0.15	0.23	mm
d_i chosen	0.20	0.20	mm
R_{ac} @ 100 kHz	118.52		mΩ
Primary Capacitance C	482		nF

low voltage winding. The comparison result is given in Fig. 10. v_{AB}, v_{CD}, i_H and i_L are HV and LV side voltage and current, separately. Both situations are with the same output voltage of 72V and output power of 1.1 kW, while the optimum one has the total system efficiency slightly improved (0.1%) to the comparison. The instrument used for the system efficiency measurement is N4L precision power analyzer. The current ringing of the optimum designed transformer is reduced, which is helpful for efficiency and EMI problems. Further reduction of the transformer capacitance requires a systematic

modeling and optimization of the capacitance network of the transformer [6].

IV. CONCLUSIONS

An improved transformer winding design method is proposed and verified in terms of ac resistance, leakage inductance, and parasitic capacitance. The impact of the winding displacement on those parasitic parameters are concretely discussed. With the comparison and understanding of the field distribution, the simple analytical equations originally for the normal winding can be applied for the displacement windings with the additional empirical coefficients. With a local optimization of capacitance, the proposed design method compresses a three-dimensional optimization to a two-dimensional problem, and achieves Pareto optimization for the ac resistance and winding capacitance. Finally, a transformer winding design case for a DAB converter is presented which leads to reduced current ringing and increased efficiency.

REFERENCES

[1] R. De Doncker, D. Divan, and M. Kheraluwala, "A three-phase soft-switched high-power-density DC/dc converter for high-power applications," vol. 27, no. 1, pp. 63–73, Jan. 1991.

[2] G. Ortiz, C. Gammeter, J. Kolar, *et al.*, "Mixed mosfet-igbt bridge for high-efficient medium-frequency dual-active-bridge converter in solid state transformers," in *Proc. IEEE Wksp. Control Model. Power Electron (COMPEL)*, 2013, pp. 1–8.

[3] S. Engel, M. Stieneker, N. Soltau, *et al.*, "Comparison of the modular multilevel DC converter and the dual-active bridge converter for power conversion in HVDC and MVdc grids," vol. 30, no. 1, pp. 124–137, Jan. 2015.

[4] J. Biela and J. W. Kolar, "Using transformer parasitics for resonant converters-a review of the calculation of the stray capacitance of transformers," vol. 44, no. 1, pp. 223–233, Jan. 2008.

[5] P. Thummala, H. Schneider, Z. Zhang, *et al.*, "Investigation of transformer winding architectures for high-voltage (2.5 kV) capacitor charging and discharging applications," vol. 31, no. 8, pp. 5786–5796, Aug. 2016.

[6] Z. Qin, Z. Shen, and F. Blaabjerg, "Modelling and analysis of the transformer current resonance in dual active bridge converters," in *Proc. IEEE Energy Conversion Congress and Exposition (ECCE)*, Sep. 2017, pp. 4520–4524.

[7] J.-P. Vandelac and P. Ziogas, "A novel approach for minimizing high-frequency transformer copper losses," vol. 3, no. 3, pp. 266–277, Jul. 1988.

[8] C. Sullivan, "Optimal choice for number of strands in a litz-wire transformer winding," vol. 14, no. 2, pp. 283–291, Mar. 1999.

[9] M. A. Bahmani and T. Thiringer, "Accurate evaluation of leakage inductance in high-frequency transformers using an improved frequency-dependent expression," vol. 30, no. 10, pp. 5738–5745, Oct. 2015.

[10] W. Schroder, "Berechnung der eigenschwingungen der doppellagigen langen spule," *Arch. Elektrotechnik*, vol. Band XI, Heft 6, pp. 203–229, 1922.

[11] M. Aghaei and S. Kaboli, "On the effect of disorder on stray capacitance of transformer winding in high-voltage power supplies," vol. 64, no. 5, pp. 3608–3618, May 2017.

[12] A. Massarini and M. K. Kazimierczuk, "Self-capacitance of inductors," vol. 12, no. 4, pp. 671–676, Jul. 1997.

[13] Elektrisola, *Technical data for enamelled copper wire by size acc. to IEC 60317*, http://www.elektrisola.com /fileadmin/webdata/english/Downloads/ELEKTRISOLA _EnCuWire_IEC_Datasheet_eng.pdff, Sep. 2017.

[14] Z. Shen, H. Wang, Y. Shen, *et al.*, "Winding design of series ac inductor for dual active bridge converters," in *Proc. IEEE Appl. Power Electron. Conf. Exposit.*, IEEE, 2018.

[15] F. Robert, P. Mathys, B. Velaerts, *et al.*, "Two-dimensional analysis of the edge effect field and losses in high-frequency transformer foils," vol. 41, no. 8, pp. 2377–2383, 2005.

[16] P. Dowell, "Effects of eddy currents in transformer windings," *Proc. Inst. Electr. Eng.*, vol. 113, no. 8, pp. 1387–1394, Aug. 1966.

[17] J. Ferreira, "Improved analytical modeling of conductive losses in magnetic components," vol. 9, no. 1, pp. 127–131, 1994.

[18] I. Villar, "Multiphysical characterization of medium-frequency power electronic transformers," PhD thesis, École Polytechnique Fédérale de Lausanne, Lausanne, Switzerland, 2010.

[19] M. Mogorovic and D. Dujic, "Medium frequency transformer leakage inductance modeling and experimental verification," in *Proc. IEEE Energy Conversion Congress and Exposition (ECCE)*, Sep. 2017, pp. 419–424.

[20] W. Hurley, E. Gath, and J. Breslin, "Optimizing the AC resistance of multilayer transformer windings with arbitrary current waveforms," vol. 15, no. 2, pp. 369–376, Mar. 2000.

[21] R. Wojda and M. Kazimierczuk, "Analytical optimization of solid–round-wire windings," vol. 60, no. 3, pp. 1033–1041, 2013.

[22] Z. Shen, Z. Li, L. Jin, *et al.*, "An ac resistance optimization method applicable for inductor and transformer windings with full layers and partial layers," in *Proc. IEEE Appl. Power Electron. Conf. Exposit.*, IEEE, 2017, pp. 2542–2548.